

# First principles search for novel ultrahard high-density carbon allotropes: hexagonal C<sub>6</sub>, C<sub>9</sub> and C<sub>12</sub>

Samir F. Matar<sup>1</sup> and Vladimir L. Solozhenko<sup>2,\*</sup>

<sup>1</sup> Lebanese German University (LGU), Sahel Alma, Jounieh, Lebanon

 <https://orcid.org/0000-0001-5419-358X>

<sup>2</sup> LSPM–CNRS, Université Sorbonne Paris Nord, 93430 Villetaneuse, France

 <https://orcid.org/0000-0002-0881-9761>

## Abstract

*Hexagonal carbon allotropes C<sub>6</sub>, C<sub>9</sub> and C<sub>12</sub> with **qtz**, **sta** and **lon** topologies, respectively, were predicted on the basis of crystal chemistry and first principles (DFT) calculations. The new allotropes are mechanically (elastic properties) and dynamically (phonons) stable phases and are characterized by ultra-high Vickers hardness, exceptionally high for **qtz** C<sub>6</sub> and C<sub>12</sub>, close to the previously studied **qtz** C<sub>3</sub>. The electronic band structures of all new allotropes show semi-conducting to insulating behavior. **lon** C<sub>12</sub> can be considered as novel “superlonsdaleite”.*

**Keywords:** Carbon allotropes; DFT; density; hardness; phonons; insulators

---

\* Corresponding author ([vladimir.solozhenko@univ-paris13.fr](mailto:vladimir.solozhenko@univ-paris13.fr))

## Introduction and context

The search and characterization of original ultra-hard carbon allotropes is an ongoing research field especially with the upstream help of modern materials research software, such as those based on evolutionary crystallography (USPEX) [1], and particle swarm optimization-based crystal structure prediction (CALYPSO) [2]. The identified carbon allotropes are compiled in the SACADA database [3] to help inform researchers of the origin of the allotropes, organized by topological categories identified with the TopCryst program [4], e.g. **dia** for diamond, **lon** for ‘lonsdaleite’ (rare hexagonal form of diamond, here identified as C<sub>12</sub>). Structures are published in the Cambridge Structural Database (CSD) (see [5] for one of the original carbon allotropes studied here, C<sub>9</sub>).

Such structural identifications require further analyses with quantum mechanical calculations to derive quantities that precisely define the desired function, such as the hardness and the mechanical (elastic properties) and dynamic (phonons) stabilities, as well as the electronic band structure. The widely recognized quantum mechanics framework of the Density Functional Theory (DFT) [6,7] is used in DFT-based computations.

The original hexagonal tricarbon C<sub>3</sub> allotrope has recently been claimed from *ab initio* investigations to be superdense and superhard [8], supporting an earlier claim for such properties [9]. Hexagonal C<sub>3</sub> is derived from silica (quartz) and assigned the **qtz** topology (SACADA **qtz** #11). The five-ring carbon topology **unj** (SACADA #29) has also been proposed for hexagonal C<sub>3</sub> [10]. Finally, we have recently investigated the linear C-C-C arrangements known for the isolated molecule in rhombohedral and hexagonal ultra-hard C<sub>3</sub> characterized by mixed sp<sup>3</sup>-sp<sup>2</sup> carbon hybridizations [11].

In this challenging context, the aim of this work is to investigate the physical properties (mechanical, dynamical, and electronic) of **qtz** C<sub>3</sub> together with structurally related novel carbon allotropes, namely **qtz** C<sub>6</sub>, **qtz** C<sub>12</sub>, **sta** C<sub>9</sub> and **lon** C<sub>12</sub>.

## Computational framework

The devised structures were subjected to geometry relaxations of the atomic positions and the lattice constants down to the ground state characterized by minimum energy. The iterative computations were performed using the DFT-based plane-wave Vienna Ab initio Simulation Package (VASP) [12,13]. The projector augmented wave (PAW) method was used for the atomic potentials [13]. The exchange X and correlation C effects (XC) were treated within a generalized gradient approximation (GGA) scheme [14]. Test calculations with a hybrid functional HSE06 [15] did not result in significant changes of the GGA results. The relaxation of the atoms to the ground state geometry was performed using a conjugate-gradient algorithm [16]. The Blöchl tetrahedron method [17] with corrections according to the Methfessel and Paxton scheme [18] was applied for geometry optimization and energy calculations, respectively. A special *k*-point sampling [19] was used to

approximate the reciprocal space Brillouin-zone (BZ) integrals. For better reliability, the optimization of the structural parameters was carried out along with successive self-consistent cycles with increasing k-mesh until the forces on the atoms were below 0.02 eV/Å and the stress components below 0.003 eV/Å<sup>3</sup>.

Mechanical stability was derived from elastic constants calculations [20]. The phonon dispersion band structures were calculated to verify the dynamic stability of the carbon allotropes. The phonon modes were calculated considering the harmonic approximation through finite displacements of the atoms around their equilibrium positions to obtain the forces from the summation over the different configurations. The phonon dispersion curves along the direction of the Brillouin zone were then obtained using the interface code "Phonopy" based on the Python language [21]. The CIF files and the structure sketches including the tetrahedral representations were generated using the VESTA software [22]. The electronic band structures and densities of states were obtained with the full-potential augmented spherical wave ASW method based on DFT using the same GGA scheme as above [23].

## Crystal chemistry

C<sub>3</sub> has a structure derived from one of the quartz varieties [10]. The structure belonging to space group *P*<sub>6</sub><sub>2</sub><sub>2</sub>, No 180 is shown in Fig. 1a in ball-and-stick and tetrahedral representations with emphasis on the tetrahedral arrangement. These representations are also applied to the other structures.

Table 1 gives literature [8] and currently calculated (in brackets) lattice constants after full unconstrained geometry optimizations. **qtz** C<sub>3</sub> is energetically less cohesive ( $E_{\text{coh}}/\text{atom} = -1.37$  eV/at.) than tricarbon formed with linear C—C—C building blocks [11] found with  $E_{\text{coh}}/\text{atom} = -1.55$  eV eV/at. Also, as a general trend, all the allotropes examined here are less cohesive than cubic and hexagonal (lonsdaleite) diamond with  $E_{\text{coh}}/\text{atom} = -2.46$  eV/atom.

By extending the carbon lattice, we identified a twice as large cell with single sixfold C positions in space group *P*<sub>6</sub><sub>5</sub><sub>2</sub>, No 179 for hexagonal C<sub>6</sub>. The calculated crystal data are given in Table 1 and the structure is shown in Fig. 1b. In **qtz** topology, C<sub>6</sub> is close to **qtz** C<sub>3</sub>, and the atomic averaged volumes are also close, although smaller in novel C<sub>6</sub>. We also include results obtained for 5-ring C<sub>6</sub> in **unf** topology such as **unj** C<sub>3</sub> (SACADA #29) [10].

Extending the stoichiometry further, novel C<sub>9</sub> with space group C<sub>9</sub> *P*<sub>6</sub><sub>4</sub><sub>2</sub>, No 179 with tetrahedral carbon was obtained (Table 1, Fig. 1c) and assigned a new (not SACADA-listed) **sta** topology using TopCryst. The structure was subsequently published in the CCDC crystallography database [5].

For the sake of completeness, in addition to the 6-fold position, space group *P*<sub>6</sub><sub>5</sub><sub>2</sub>, No 179 has a 12-fold particular (12c) x, y, z position, which was considered for devising extended C<sub>12</sub>

stoichiometry. After full geometry relaxation down to the energy minimum, the ground state parameters are given in Table 1, and the structure is shown in Fig. 3e. The tetrahedral arrangement is more regular than in C<sub>3</sub>, C<sub>6</sub>, C<sub>9</sub> and **qtz** C<sub>12</sub>, and was found to be related to diamond-like. In fact, further analysis of the topology of C<sub>12</sub> revealed it to be of the **lon** type, i.e., lonsdaleite (hexagonal diamond). Deeper crystallographic characterization led to lonsdaleite's space group *P6<sub>3</sub>/mmc*, No 194 for C<sub>12</sub> characterized by a splitting of the (12c) site into three (4f) sites with parameters given in the last column of Table 1. Consequently, we assign to novel C<sub>12</sub> the label of “*superlonsdaleite*”. Note that space group No 179 is a subgroup of space group No 194.

Comparing the volumes of the four different carbon stoichiometries can be done by averaging them per atom. Table 1 shows that the volumes of C<sub>3</sub>, C<sub>6</sub> and **qtz** C<sub>12</sub> are smaller than the values for C<sub>9</sub> and C<sub>12</sub>, which would lead one to expect higher densities for them, as discussed in the sections on hardness and densities.

### **Mechanical properties from elastic constants**

The analysis of the mechanical behavior was subsequently carried out with the elastic properties by performing finite distortions of the lattice. The system is then fully described by the bulk (*B*) and the shear (*G*) moduli obtained by averaging the elastic constants using Voigt's method [20] based on a uniform strain.

The calculated sets of elastic constants C<sub>ij</sub> (i and j correspond to directions) are given in Table 2. All C<sub>ij</sub> values are positive. The elastic constants of **lon** C<sub>12</sub> have the largest magnitudes, close to those of diamond [24]. The structurally related C<sub>3</sub> and C<sub>6</sub> have slightly smaller magnitudes. C<sub>9</sub> has large C<sub>ij</sub> values, but they remain smaller than all the other carbon allotropes studied.

The bulk *B<sub>V</sub>* and the shear *G<sub>V</sub>* moduli were then obtained from the equations corresponding to the hexagonal system [25]:

$$B_V = 1/9 \{2(C_{11} + C_{12}) + 4C_{13} + C_{33}\}$$

$$G_V = 1/30 \{C_{11} + C_{12} + 2C_{33} - 4C_{13} + 12C_{44} + 6(C_{11} - C_{12})\}$$

The last two columns of Table 2 show the obtained *B<sub>V</sub>* and *G<sub>V</sub>*. C<sub>12</sub> has the largest values, close to the accepted values for diamond, *B<sub>V</sub>* = 445 GPa and *G<sub>V</sub>* = 550 GPa [26]. The other allotropes also have large bulk and shear moduli values, close to diamond, especially C<sub>3</sub> and C<sub>6</sub>, while C<sub>9</sub> has the smallest values.

Vickers hardness (*H<sub>V</sub>*) has been predicted using four contemporary theoretical models. The thermodynamic (T) model [27], which is based on thermodynamic properties and crystal structure, shows surprising agreement with available experimental data [28] and is therefore recommended for hardness evaluation of superhard and ultrahard phases [29]. The Lyakhov-Oganov (LO) approach [30] takes into account the topology of the crystal structure, the strength of covalent bonding, the

degree of ionicity and directionality; however, in the case of ultrahard phases of light elements, this model gives underestimated hardness values [28,29]. Two empirical models, Mazhnik-Oganov (MO) [31] and Chen-Niu (CN) [32], use the elastic properties. Fracture toughness ( $K_{Ic}$ ) has been evaluated within the Mazhnik-Oganov model [31]. The results for the currently proposed hexagonal carbon allotropes and others from the literature are summarized in Tables 3 and 4.

Table 3 gives general information on the crystal structures, densities, hardness and bulk moduli according to the thermodynamic model. Focusing on the density, there is a clear evidence of higher densities for the **qtz** allotropes ( $C_3$ ,  $C_6$  and  $C_{12}$ ) compared to other carbon allotropes. The lowest density is observed for the 5-ring open structure of **unj**  $C_6$  [10,33].

The analysis of all the data (Tables 3 and 4) allows us to conclude that the high density gives rise to high hardness values, which are the highest for the **qtz** allotropes mentioned above; but this does not allow us to say that their hardness is higher than that of diamond. Finally, the bulk moduli are also higher for the **qtz**  $C_3$ ,  $C_6$  and  $C_{12}$  allotropes, but remain within the limits of diamond/lonsdaleite.

### **Dynamic properties from the phonons**

An important criterion of phase stability is obtained from the phonon's properties. Phonons are quanta of vibrations; their energy is quantized by the Planck constant 'h' which is used in its reduced form  $\hbar$  ( $\hbar = h/2\pi$ ), giving the phonons energy:  $E = \hbar\omega$  (frequency:  $\omega$ )

All four carbon allotropes were subjected to phonon studies to determine their respective dynamic properties. Fig. 2 shows the phonon bands. In the horizontal direction, the bands develop along the main lines of the hexagonal Brillouin zone (reciprocal k-space). The vertical direction shows the frequencies  $\omega$ , which are given in terahertz (THz) units.

There are  $3N-3$  optical modes found at higher energy than three acoustic modes, starting from zero energy ( $\omega = 0$ ) at the  $\Gamma$  point, center of the Brillouin zone (BZ), up to a few terahertz. They correspond to the lattice rigid translation modes of the crystal (two transverse and one longitudinal). The remaining bands correspond to the optical modes and culminating at  $\omega \sim 40$  THz in  $C_{12}$ , a value observed for diamond by Raman spectroscopy [36].

Focusing on  $C_3$ , the phonons have a negative frequency (\*) along  $\Gamma-A$  i.e., along the vertical direction of the BZ indicating instability towards a transient state, i.e., the structure could be unstable, and a possible phase transition could occur. However, we note that in the "qtz"  $C_3$  paper [9] the authors claimed all positive phonons without showing corresponding band structures. While we do not question their results, we point out that in the same calculation protocols for all four carbon forms, the other carbon stoichiometries show no negative phonons and they are considered to be dynamically stable. We propose that the extension of the carbon stoichiometry in the presently studied series is a stabilizing factor of the carbon structure.

## Electronic band structures and density of states

Using the crystal parameters in Table 1, the electronic band structures were obtained using the all-electrons DFT-based augmented spherical method (ASW) [23] and are shown in Figure 3. The bands develop along the main directions of the primitive tetragonal Brillouin zones. As all four systems are characterized with a band gap between the valence band (VB) and the empty conduction band (CB), the energy reference along the vertical energy axis is with the respect to the top of the VB.

The band structures of  $C_3$  and  $C_6$  are different, although they are similar in shape. The lowest CB band is at M in both. For the VB, however, the highest band is found at A point in  $C_3$ , whereas in  $C_6$  the highest valence band is at the  $\Gamma$  point, as is more commonly found. In  $C_9$  the band gap is small  $\sim 0.5$  eV, indicating semiconducting behavior. Finally, the largest band gap is observed for the diamond-like  $C_{12}$  with a magnitude close to 4 eV with indirect  $\Gamma_{VB}$ - $M_{CB}$  character.

## References

- [1] A.R. Oganov, Crystal structure prediction: reflections on present status and challenges. *Faraday Discuss.* **211** (2018) 643-660.
- [2] Y. Wang, J. Lv, L. Zhu, Y. Ma, CALYPSO: A method for crystal structure prediction. *Comput. Phys. Commun.* **183** (2012) 2063-2070.
- [3] R. Hoffmann, A.A. Kabanov, A.A. Golov, D.M. Proserpio, *Homo Citans* and carbon allotropes: For an ethics of citation. *Angew. Chem. Int. Ed.* **55** (2016) 10962-10976; SACADA database (*Samara Carbon Allotrope Database*), [www.sacada.info](http://www.sacada.info)
- [4] A.P. Shevchenko, A.A. Shabalin, I.Yu. Karpukhin, V.A. Blatov, Topological representations of crystal structures: generation, analysis and implementation in the *TopCryst* system. *Sci Technol Adv Mat.* **2** (2022) 250-265.
- [5] S.F. Matar, CCDC 2233635: Crystal Structure Determination, 2022, DOI: [10.5517/ccdc.esd.cc2dz8rf](https://doi.org/10.5517/ccdc.esd.cc2dz8rf)
- [6] P. Hohenberg, W. Kohn, Inhomogeneous electron gas. *Phys. Rev. B* **136** (1964) 864-871.
- [7] W. Kohn, L.J. Sham, Self-consistent equations including exchange and correlation effects. *Phys. Rev. A* **140** (1965) 1133-1138.
- [8] B. Luo, L. Wu, Z. Zhang, G. Li, E. Tian, A triatomic carbon and derived pentacarbides with superstrong mechanical properties. *iScience* **25** (2022) 104712.
- [9] Q. Zhu, A.R. Oganov, M.A. Salvadó, P. Pertierra, A.O. Lyakhov, Denser than diamond: *Ab initio* search for superdense carbon allotropes. *Phys. Rev. B* **83** (2011) 193410.
- [10] L. Öhrström, M. O'Keeffe, Network topology approach to new allotropes of the group 14 elements. *Z. Kristallogr.* **228** (2013) 343-346.
- [11] S.F. Matar, J. Etourneau, V.L. Solozhenko, First-principles investigations of tricarbon: From the isolated C<sub>3</sub> molecule to a novel ultra-hard anisotropic solid. *Carbon Trends.* **6** (2022) 100132.
- [12] G. Kresse, J. Furthmüller, Efficient iterative schemes for ab initio total-energy calculations using a plane-wave basis set. *Phys. Rev. B* **54** (1996) 11169.
- [13] G. Kresse, J. Joubert, From ultrasoft pseudopotentials to the projector augmented wave. *Phys. Rev. B* **59** (1994) 1758-1775.
- [14] J. Perdew, K. Burke, M. Ernzerhof, The Generalized Gradient Approximation made simple. *Phys. Rev. Lett.* **77** (1996) 3865-3868.
- [15] J. Heyd, G.E. Scuseria, M. Ernzerhof, Hybrid functionals based on a screened Coulomb potential. *J. Chem. Phys.* **124** (2006) 219906.

- [16] W.H. Press, B.P. Flannery, S.A. Teukolsky, W.T. Vetterling, *Numerical Recipes*, 2<sup>nd</sup> ed., Cambridge University Press: New York, USA, 1986.
- [17] P.E. Blöchl, O. Jepsen, O.K. Anderson, Improved tetrahedron method for Brillouin-zone integrations. *Phys. Rev. B* **49** (1994) 16223-16233.
- [18] M. Methfessel, A.T. Paxton, High-precision sampling for Brillouin-zone integration in metals. *Phys. Rev. B* **40** (1989) 3616-3621.
- [19] H.J. Monkhorst, J.D. Pack, Special k-points for Brillouin Zone integration. *Phys. Rev. B* **13** (1976) 5188-5192.
- [20] W. Voigt, Über die Beziehung zwischen den beiden Elasticitätsconstanten isotroper Körper. *Annal. Phys.* **274** (1889) 573-587.
- [21] A. Togo, I. Tanaka, First principles phonon calculations in materials science. *Scr. Mater.* **108** (2015) 1-5.
- [22] K. Momma, F. Izumi, VESTA 3 for three-dimensional visualization of crystal, volumetric and morphology data. *J. Appl. Crystallogr.* **44** (2011) 1272-1276.
- [23] V. Eyert, Basic notions and applications of the augmented spherical wave method. *Int. J. Quantum Chem.* **77** (2000) 1007-1031.
- [24] R.S. Krishnan, V. Chandrasekharan, E.S. Rajagopal, The four elastic constants of diamond. *Nature* **182** (1958) 518-520.
- [25] D.C. Wallace, *Thermodynamics of crystals*. New York, USA: John Wiley and Sons; 1972.
- [26] V.V. Brazhkin, V.L. Solozhenko, Myths about new ultrahard phases: Why materials that are significantly superior to diamond in elastic moduli and hardness are impossible. *J. Appl. Phys.* **125** (2019) 130901.
- [27] V.A. Mukhanov, O.O. Kurakevych, V.L. Solozhenko, The interrelation between hardness and compressibility of substances and their structure and thermodynamic properties. *J. Superhard Mater.* **30** (2008) 368-378.
- [28] S.F. Matar, V.L. Solozhenko, Crystal chemistry and ab initio prediction of ultrahard rhombohedral B<sub>2</sub>N<sub>2</sub> and BC<sub>2</sub>N. *Solid State Sci.* **118** (2021) 106667.
- [29] V.L. Solozhenko, S.F. Matar, Prediction of novel ultrahard phases in the B–C–N system from first principles: Progress and problems. *Materials* **16** (2023) 886.
- [30] A.O. Lyakhov, A.R. Oganov, Evolutionary search for superhard materials: Methodology and applications to forms of carbon and TiO<sub>2</sub>. *Phys. Rev. B* **84** (2011) 092103.
- [31] E. Mazhnik, A.R. Oganov, A model of hardness and fracture toughness of solids. *J. Appl. Phys.* **126** (2019) 125109.

- [32] X.Q. Chen, H. Niu, D. Li, Y. Li, Modeling hardness of polycrystalline materials and bulk metallic glasses. *Intermetallics* **19** (2011) 1275-1281.
- [33] M. O'Keeffe, G.B. Adams, O.F. Sankey, Predicted new low energy forms of carbon. *Phys Rev. Lett.* **68** (1992) 2325-2328.
- [34] P.D. Ownby, X. Yang, J. Liu, Calculated X-ray diffraction data for diamond polytypes. *J. Am. Ceram. Soc.* **75** (1992) 1876-1883.
- [35] N. Bindzus, T. Straasø, N. Wahlberg, J. Becker, L. Bjerg, N. Lock, A.-C. Dippel, B.B. Iversen, Experimental determination of core electron deformation in diamond. *Acta Cryst. A* **70** (2014) 39-48.
- [36] R.S. Krishnan, Raman spectrum of diamond, *Nature* **155** (1945) 171.

**Table 1** Crystal structure parameters of hexagonal carbon allotropes.

	$a$ (Å)	$c$ (Å)	$V_{cell}$ (Å <sup>3</sup> )	$V_{atom}$ (Å <sup>3</sup> )	Position
<b>qtz</b> C <sub>3</sub> <sup>#180</sup> [8] *	2.6010 (2.5975)	2.7866 (2.7925)	16.326 (16.316)	5.44	C(3c) $\frac{1}{2}, 0, 0$
<b>qtz</b> C <sub>6</sub> <sup>#179</sup>	2.5975	5.5858	32.63	5.43	C(6a) 0.498, 0, 0
<b>sta</b> C <sub>9</sub> <sup>#181</sup>	2.5889	8.6153	50.57	5.64	C <sub>1</sub> (3a) 0, 0, 0 C <sub>2</sub> (6f) 0, 0, 0.2227
<b>qtz</b> C <sub>12</sub> <sup>#181</sup>	5.1949	2.7953	65.27	5.44	C <sub>1</sub> (6g) 0.25, 0, 0 C <sub>2</sub> (6i) 0.25, 0.5, 0
<b>lon</b> C <sub>12</sub> <sup>#179</sup>	2.5046	12.498	67.97	5.66	C(12c) $\frac{2}{3}, \frac{1}{3}, 0.0210$
<b>lon</b> C <sub>12</sub> <sup>#194</sup>	2.5046	12.498	67.97	5.66	3 × C(4f) $\frac{2}{3}, \frac{1}{3}, z$ $z_1 = 0.0210$ $z_2 = 0.1457$ $z_3 = 0.8124$

\* The values in brackets have been calculated in the present work.

**Table 2** Elastic constants  $C_{ij}$  and Voigt values of bulk ( $B_V$ ) and shear ( $G_V$ ) moduli of hexagonal carbon allotropes (all values are in GPa).

	$C_{11}$	$C_{12}$	$C_{13}$	$C_{33}$	$C_{44}$	$B_V$	$G_V$
<b>qtz</b> $C_3$ <sup>#180</sup>	1196	78	64	1162	559	439	558
<b>qtz</b> $C_6$ <sup>#179</sup>	1186	88	64	1162	549	441	550
<b>sta</b> $C_9$ <sup>#181</sup>	1031	170	62	1081	430	415	448
<b>qtz</b> $C_{12}$ <sup>#181</sup>	1158	86	54	1147	536	428	540
<b>lon</b> $C_{12}$ <sup>#179</sup>	1211	107	11	1338	552	446	573
<b>lon</b> $C_{12}$ <sup>#194</sup>	1211	107	11	1338	552	446	573

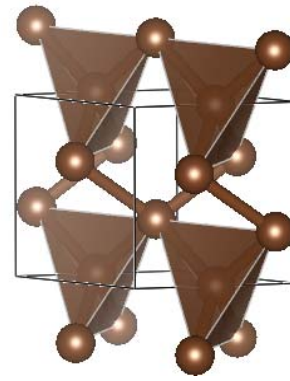
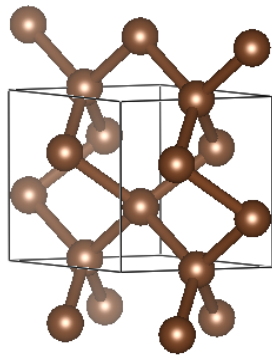
**Table 3** Vickers hardness ( $H_V$ ) and bulk moduli ( $B_0$ ) of hexagonal carbon allotropes calculated in the framework of the thermodynamic model of hardness [27] ( $pw$  = present work).

	Space group	$a = b$ (Å)	$c$ (Å)	$\rho$ (g/cm <sup>3</sup> )	$H_V$ (GPa)	$B_0$ (GPa)
<b>qtz</b> C <sub>3</sub> #180 [9]	$P6_222$	2.605	2.801	3.635	101 <sup><i>pw</i></sup>	458 <sup><i>pw</i></sup>
<b>qtz</b> C <sub>3</sub> #180 [8]	$P6_222$	2.613	2.811	3.600	100 <sup><i>pw</i></sup>	454 <sup><i>pw</i></sup>
<b>qtz</b> C <sub>3</sub> #180 [ <i>pw</i> ]	$P6_222$	2.6010	2.7866	3.665	101	462
<b>unj</b> C <sub>6</sub> #178 [33]	$P6_122$	3.5626	3.3673	3.233	90 <sup><i>pw</i></sup>	407 <sup><i>pw</i></sup>
<b>qtz</b> C <sub>6</sub> #179	$P6_522$	2.5975	5.58585	3.666	102	462
<b>sta</b> C <sub>9</sub> #181	$P6_422$	2.5889	8.6153	3.590	99	452
<b>lon</b> C <sub>12</sub> #179	$P6_522$	2.5046	12.498	3.525	98	444
<b>qtz</b> C <sub>12</sub> #181	$P6_422$	5.1942	2.7925	3.668	102	462
<b>lon</b> C <sub>12</sub> #179	$P6_522$	2.5046	12.498	3.525	98	444
<b>lon</b> C <sub>12</sub> #194	$P6_3/mmc$	2.5046	12.498	3.525	98	444
Lonsdaleite	$P6_3/mmc$	2.5221 <sup>[34]</sup>	4.1186 <sup>[34]</sup>	3.5164	97	443
Diamond	$Fd-3m$	3.56661 <sup>[35]</sup>		3.5169	98	445 <sup>[26]</sup>

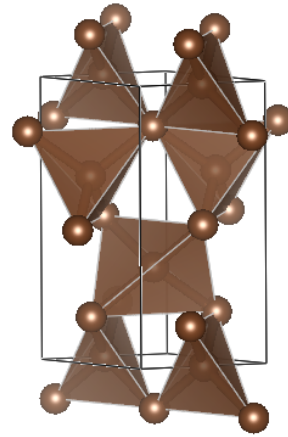
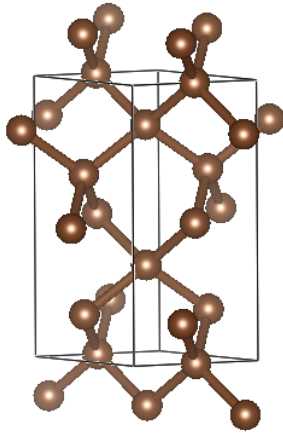
**Table 4** Mechanical properties of hexagonal carbon allotropes: Vickers hardness ( $H_V$ ), bulk modulus ( $B$ ), shear modulus ( $G$ ), Young's modulus ( $E$ ), Poisson's ratio ( $\nu$ ) and fracture toughness ( $K_{Ic}$ )

	$H_V$				$B$		$G_V$	$E^*$	$\nu^*$	$K_{Ic}$
	T	LO	MO	CN	$B_0$	$B_V$				
	GPa									
<b>qtz</b> C <sub>3</sub> <sup>#180</sup> [9]	101 <sup>pw</sup>	89 <sup>pw</sup>	–	–	458 <sup>pw</sup>	433	–	–	–	–
<b>qtz</b> C <sub>3</sub> <sup>#180</sup> [8]	100 <sup>pw</sup>	89 <sup>pw</sup>	99 <sup>pw</sup>	98 <sup>pw</sup>	454 <sup>pw</sup>	416	521	1103	0.06 <sup>pw</sup>	5.9 <sup>pw</sup>
<b>qtz</b> C <sub>3</sub> <sup>#180</sup> [pw]	101	90	106	104	462	439	558	1176	0.054	6.4
<b>unj</b> C <sub>6</sub> <sup>#178</sup> [33]	90 <sup>pw</sup>	82 <sup>pw</sup>	–	–	407 <sup>pw</sup>	–	–	–	–	–
<b>qtz</b> C <sub>6</sub> <sup>#179</sup>	102	90	105	101	462	441	550	1165	0.060	6.4
<b>sta</b> C <sub>9</sub> <sup>#181</sup>	99	88	83	75	452	416	448	989	0.104	5.5
<b>qtz</b> C <sub>12</sub> <sup>#181</sup>	102	90	103	101	462	428	540	1140	0.056	6.2
<b>lon</b> C <sub>12</sub> <sup>#179</sup>	98	90	109	107	444	446	573	1204	0.050	6.6
<b>lon</b> C <sub>12</sub> <sup>#194</sup>	98	90	109	107	444	446	573	1204	0.050	6.6
Lonsdaleite	97	90	99	94	443	432	521	1115	0.070	6.2
Diamond	98	90	100	93	445 <sup>[26]</sup>		530 <sup>[26]</sup>	1138	0.074	6.4

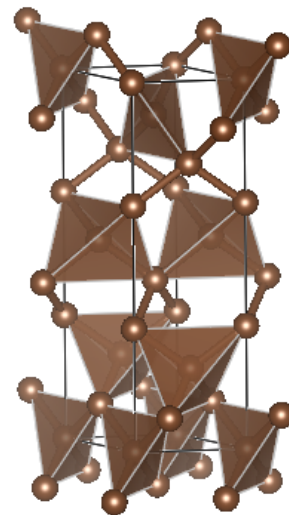
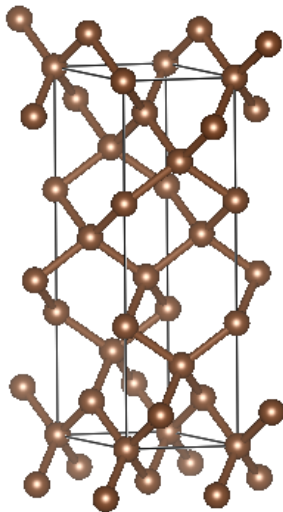
\*  $E$  and  $\nu$  values calculated using isotropic approximation



(a)



(b)



(c)

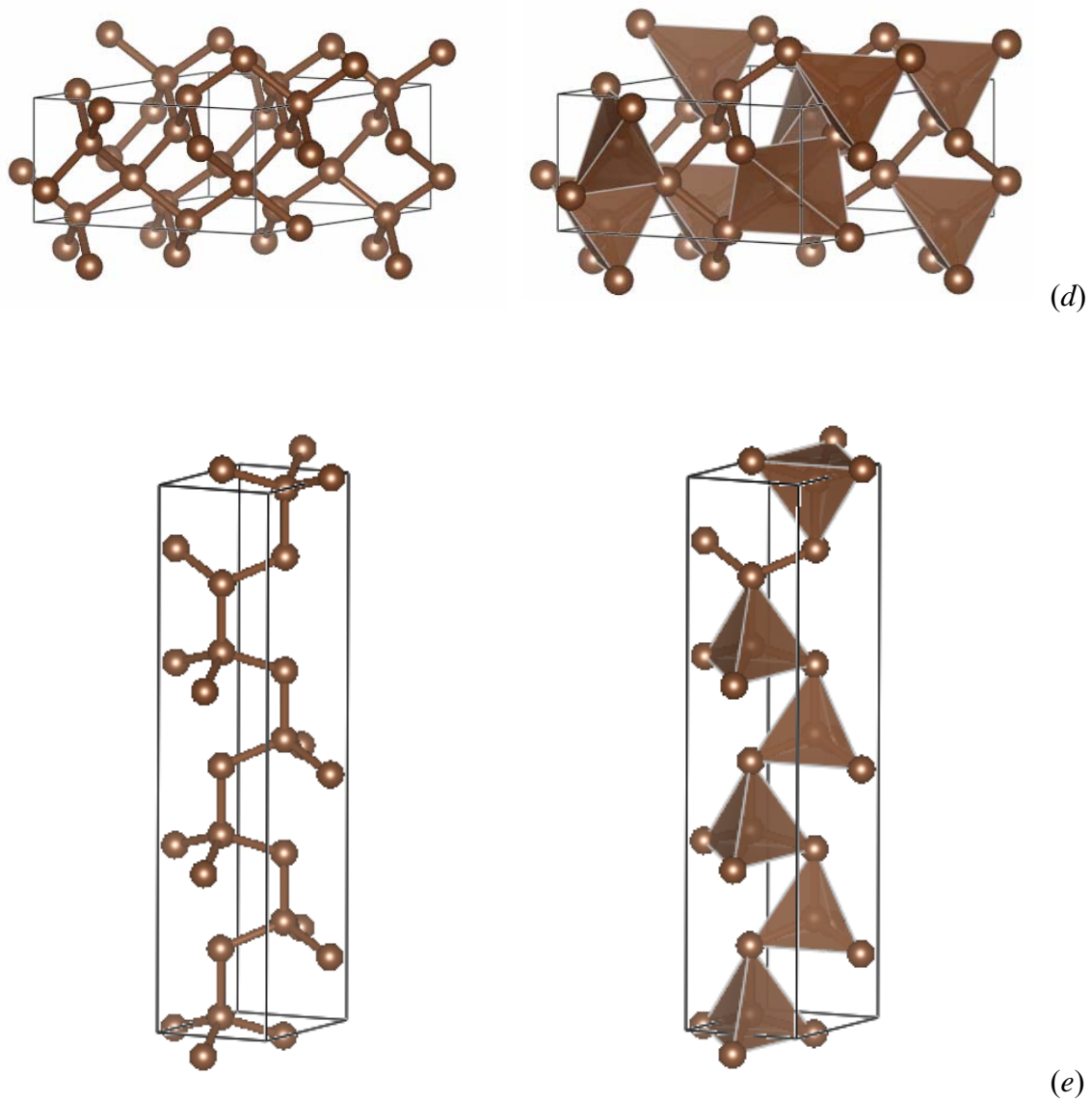
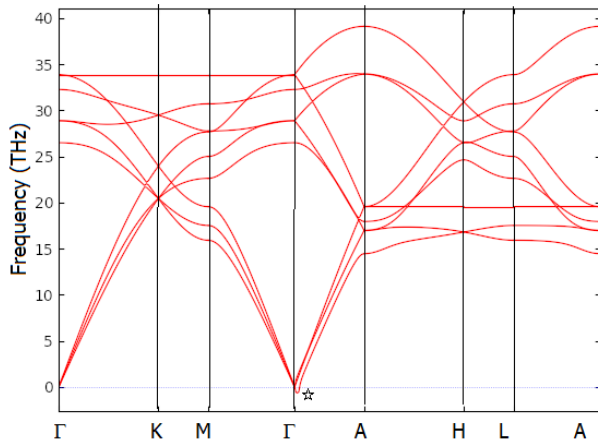
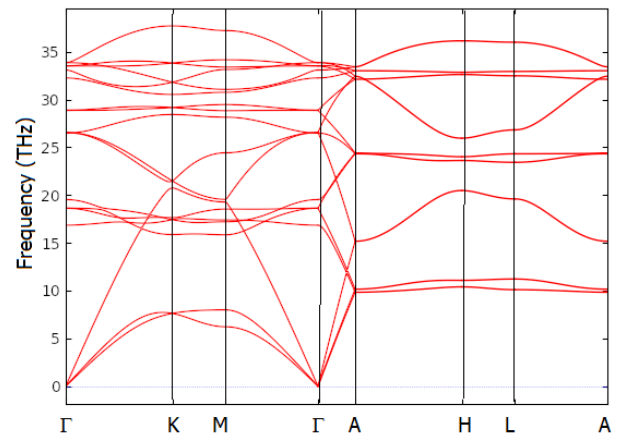


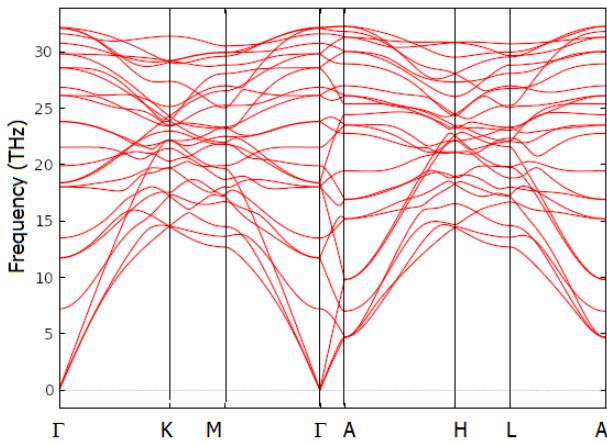
Figure 1. Sketches of the crystal structures of hexagonal carbon allotropes (with polyhedral representation): (a) **qtz**  $C_3$  [9]; (b) **qtz**  $C_6$ ; (c) **sta**  $C_9$ ; (d) **qtz**  $C_{12}$ ; (e) **lon**  $C_{12}$ .



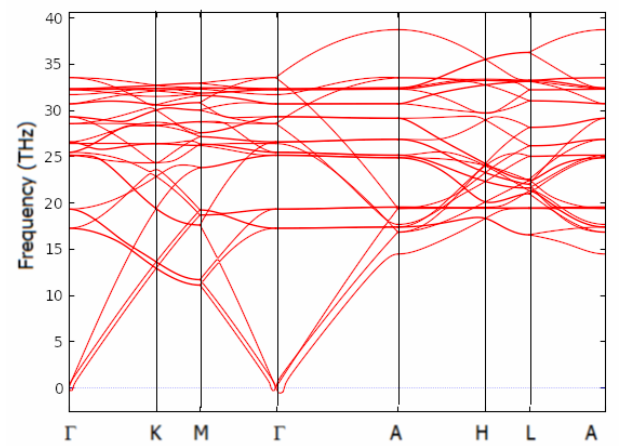
(a)



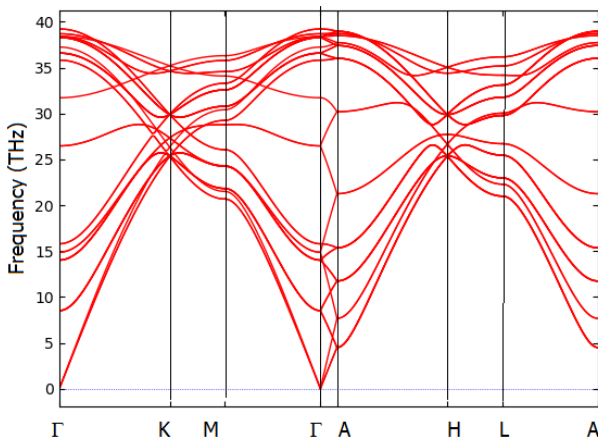
(b)



(c)



(d)



(e)

Figure 2. Phonon band structures of hexagonal carbon allotropes: (a) **qtz** C<sub>3</sub> (#180); (b) **qtz** C<sub>6</sub> (#179); (c) **sta** C<sub>9</sub> (#181); (d) **qtz** C<sub>12</sub> (#181); (e) **lon** C<sub>12</sub> (#194).

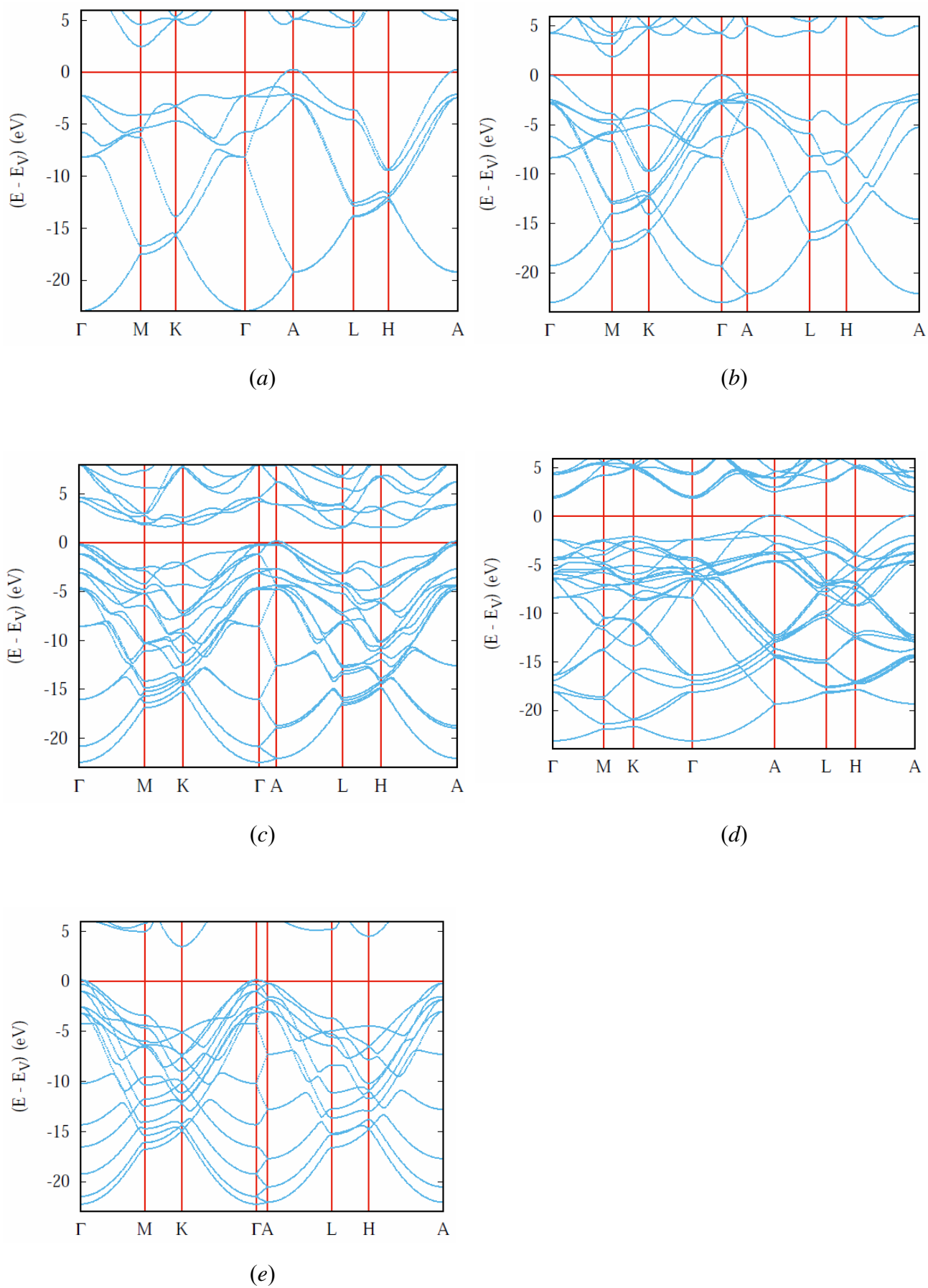


Figure 3. Electronic band structures of hexagonal carbon allotropes: (a) **qtz C<sub>3</sub>** (#180); (b) **qtz C<sub>6</sub>** (#179); (c) **sta C<sub>9</sub>** (#181); (d) **qtz C<sub>12</sub>** (#181); (e) **lon C<sub>12</sub>** (#194).